Physics Letters A ••• (••••) •••–•••

Contents lists available at ScienceDirect

Physics Letters A

www.elsevier.com/locate/pla

Detecting the Anomalous Quantum Hall phase under magnetic field

Yi-Xiang Wang [a,*], Fu-Xiang Li [b], Jie Cao [c], Ya-Min Wu [a]

[a] School of Science, Jiangnan University, Wuxi 214122, China
[b] Department of Physics, Texas A&M University, College Station, TX 77843-4242, United States
[c] National Laboratory of Solid State Microstructures and Department of Physics, Nanjing University, Nanjing 210093, China

ARTICLE INFO

Article history:
Received 29 March 2014
Received in revised form 7 May 2014
Accepted 14 May 2014
Available online xxxx
Communicated by R. Wu

Keywords:
Quantum hall effect
Excitation fraction
Square lattice

ABSTRACT

Detecting the charming topological phase has been an ongoing topic. In this work, we take the square lattice as an example and try to detect the anomalous quantum Hall (AQH) phase under magnetic field. We analyze the topological energy levels of the system, the quantum Hall effect and quantum valley Hall effect, and the number of scattered electrons after a laser pulse, from which the unambiguous signals to characterize the AQH phases can be obtained. Meanwhile the corresponding valley polarizations of electrons are investigated. Our study opens new perspectives for the applications of valleytronics in the future.

1. Introduction

Topological phases of matter which have been an interesting topic in condensed matter in recent years [1,2] are characterized by the gapless edge states and quantized charge transport. Due to their novel properties, the topological phases exhibit potential applications in the spintronics [3] and valleytronics [4] which aim at controlling the spin and valley degree of freedom of electrons for future use as data storage and transmission in semiconductor.

The study of topological phase originates from the understanding of the integer quantum Hall effect (IQHE) in which the magnetic field breaks the time reversal symmetry (TRS) of the system. In Haldane's seminal paper [5], the periodic magnetic flux on the honeycomb lattice is introduced which vanishes in a plaquette to break the TRS, therefore the anomalous quantum Hall effect (AQHE) appears without the Landau levels (LLs). Besides that, the AQHE can be realized in the spinless two-dimensional (2D) square lattice when certain conditions are satisfied [6,7]. The essence is to endow nonequivalent masses to electrons in different valleys which opens the excitonic gap and breaks the valley symmetry.

When an external magnetic field is applied on the two-dimensional electron gas (2DEG), it will split the original continuous Bloch bands into discrete Landau levels (LLs), which results in the Hofstader butterfly spectrum [8]. The Hall conductance is quantized when the Landau subbands below the Fermi surface are filled. Haldane first proved the existence of AQHE in the limit of vanishingly small magnetic field with the Streda formula [5]. In this work, we try to detect the AQH phase under magnetic field and take the square lattice as an example. The square lattice can also support the existence of Weyl semimetal [9,10] and 2π-flux topological semimetal in different parameter ranges. In these different quantum states, a novel symmetry called the hidden symmetry is proposed which corresponds to the antiunitary composite operation [11].

In experiment, the cold atom technique opens the path to simulate the topological phases with precisely controlled parameters [12]. The synthetic magnetic field [13] and spin–orbit coupling (SOC) [14] have been realized in cold atoms with suitably arranged lasers, especially the recent progresses in realizing the extremely strong magnetic flux which can be of $(0.1 \sim 1)\frac{h}{e}$ in a unit cell with Raman-assisted lasers [15–17] where $\frac{h}{e}$ is the elementary flux quantum. In terms of these developments, an important issue is to identify the observables which can provide evident signatures of the topological phases [7,18]. In simulating the AQH phase with the cold atom, the square lattice model is more feasible than Haldane's honeycomb lattice model [6,19] as the periodic magnetic flux plays a minor role in square lattice. With a well-designed laser field probe, the chiral edge states with specific property in the Hofstadter optical lattice can be captured by the Bragg spectra that is sensitive to angular momentum [20].

Here we provide a detailed account on three striking manifestations of the interplay between the AQH phase in square lattice and the magnetic field, which can be used to detect the AQH phase. First we analyze the topological structure of energy bands and LLs in the system when the magnetic field is absent or present. The wavefunctions of the bands at the Dirac points and the chiralities of $n = 0$ LLs in both valleys are different in topologically trivial

* Corresponding author.

http://dx.doi.org/10.1016/j.physleta.2014.05.012

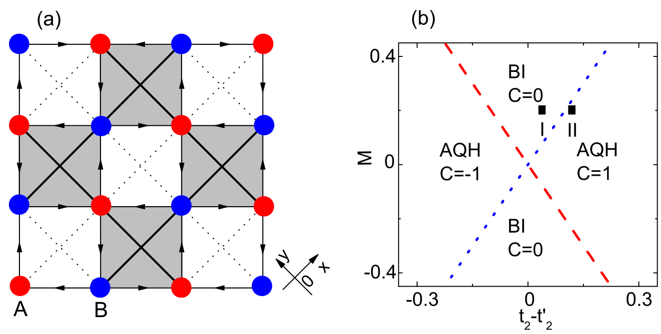

Fig. 1. (Color online.) (a) Schematic plot of 2D square lattice which consists of two sublattice A (red) and B (blue). The darker and lighter plaquettes represent the staggered magnetic flux while the solid and dashed lines are for the anisotropy NNN hoppings. The arrows denote the phase gauge that we choose to represent the staggered magnetic flux. (b) The phase diagram in parametric space $(M, t_2 - t_2')$ where the Chern number is shown. The red dashed (blue dotted) line marks the sign inversion of m_+ (m_-).

and nontrivial phases. Next we study the quantum Hall response of the system as well as the quantum valley Hall effect (QVHE) [4,21], where the Dirac fermions in different valleys flow to opposite transverse edges when an in-plane electric field is applied. The Hall conductance and valley Hall conductance at the charge neutral point (CNP) can characterize the different topological phases. After the application of a short laser pulse, we investigate the excited electron number and the accompanied valley polarization. From the change of the number of scattered electrons, the different topological phases can be further identified. Our work may provide new perspectives to control the AQH phase and the valley-polarized electrons with the help of magnetic field, which are of particular interests for valleytronics [22] in the future.

2. Model

We start from the square lattice which consists of two sublattices A and B and the staggered magnetic flux in neighboring plaquettes as shown in Fig. 1(a). The square lattice has a lattice spacing a. When a uniform magnetic field is applied on the system along z-axis $\mathbf{B} = B\mathbf{e}_z$, it will cause the hopping integrals to acquire the Peierls phase, which can be encoded by the minimum substitution to the momentum $\mathbf{p} \to \mathbf{p} + e\mathbf{A}$ where $\mathbf{A}$ is the vector potential. Thus any hopping process from site $\mathbf{r}_i$ to $\mathbf{r}_j$ acquires the phase factor $e^{i\phi_{ij}}$, in which $\phi_{ij} = 2\pi \frac{e}{\hbar} \int_{\mathbf{r}_i}^{\mathbf{r}_j} \mathbf{A} \cdot d\mathbf{r}$. We can express the magnetic field as $B = \frac{\phi}{2a^2} \frac{h}{e}$ and the dimensionless quantity ϕ is in unit of $\frac{h}{e}$ which gives the magnetic flux penetrating a unit cell whose area is $2a^2$. For convenience, we take $\phi = \frac{1}{p}$ where p is an integer so that the magnetic flux is commensurate with the lattice structure [23]. In the frame of second-quantization, the relevant tight-binding Hamiltonian under magnetic field takes the form:

$$\hat{H}_0 = M \sum_i (\hat{a}_i^+ \hat{a}_i - \hat{b}_i^+ \hat{b}_i) - t_1 \sum_{\langle i,j \rangle} (e^{i\varphi_{ij} + i\phi_{ij}} \hat{a}_i^+ \hat{b}_j + \text{H.c.}) - \sum_{\langle\langle ij \rangle\rangle} t_{i,j} e^{i\phi_{ij}} (\hat{a}_i^+ \hat{a}_j + \hat{b}_i^+ \hat{b}_j), \tag{1}$$

where $\hat{a}_i(\hat{a}_i^+)$ and $\hat{b}_i(\hat{b}_i^+)$ are the annihilation (creation) operators on site R_i in sublattice A and B, respectively. The staggered onsite energy M on different sublattice breaks the inversion symmetry. t_1 is the isotropy nearest-neighbor (NN) hopping integral and t_{ij} is the anisotropy next-nearest-neighbor (NNN) hopping integral, which takes t_2 in one direction (solid diagonal lines in Fig. 1(a)) and t_2' in the perpendicular direction (dashed diagonal lines). φ_{ij} is the Peierls phase from site i to its NN j which takes φ for the hopping direction along the arrows in the figure. Here we do not consider the spin and neglect the Zeeman effect. Note that although the staggered magnetic flux φ does not break the macroscopic TRS of the system [24], it plays an essential role in forming the isotropic Dirac cones and therefore is taken to be $\frac{\pi}{4}$. The two-sublattice square lattice resembles the heavy-fermion system [25] and the $d + id$ model in high-temperature superconductors [26,27]. A little simplified model was ever used to study the redistribution of Chern numbers which associates with the LL movements [28].

3. Main results

3.1. Band structures and LLs

First we analyze the topological structure of the system. When the magnetic field is absent, we can expand $\hat{H}_0$ around two unequivalent Dirac points $\mathbf{K} = \frac{\pi}{\sqrt{2}a}(1, 0)$ and $\mathbf{K}' = \frac{\pi}{\sqrt{2}a}(0, 1)$ to get the low-energy Hamiltonians of Dirac-type:

$$\hat{H}_+ = v_F (p_x \sigma_x - p_y \sigma_y) + m_+ \sigma_z, \tag{2}$$

$$\hat{H}_- = v_F (p_y \sigma_x - p_x \sigma_y) + m_- \sigma_z. \tag{3}$$

The Pauli matrices σ_i $(i = x, y, z)$ act on the sublattice space. $v_F = \frac{2\sqrt{2}at_1}{\hbar}$ is the Fermi velocity and $m_{\alpha=\pm} = M + 2\alpha(t_2 - t_2')$ give the electron mass in valley α in which the valley index $\alpha = +1(-1)$ for the Dirac point $\mathbf{K}$ ($\mathbf{K}'$). Here the staggered onsite energy and the anisotropy NNN hoppings break the valley symmetry which make the valley-polarized electron possible.

In spinless system, the topological phase can be characterized by the Chern number which is the integration of the Berry curvature in the momentum space as $C = \frac{1}{4\pi} \int d\mathbf{k} \frac{\partial \hat{\mathbf{h}}}{\partial k_x} \times \frac{\partial \hat{\mathbf{h}}}{\partial k_y} \cdot \hat{\mathbf{h}}$, where $\hat{\mathbf{h}} = \frac{\mathbf{h}}{|\mathbf{h}|}$ is the unit Hamiltonian vector. Due to the different combinations of the momentum and Pauli matrix in $\hat{H}_+$ and $\hat{H}_-$, their Chern number components have different signs so that the total Chern number is $C = \frac{1}{2}[\text{sgn}(m_+) - \text{sgn}(m_-)]$ [6]. The phase diagram of Chern number is shown in Fig. 1(b), in which the red dashed (blue dotted) line marks the sign inversion of m_+ (m_-). The inversion of the electron mass plays a decisive role in the phase transition and can drive the formation of topologically protected edge modes. When $|M| < |2(t_2 - t_2')|$, m_+ and m_- take opposite signs, so the Chern number is nonvanishing and the system lies in the nontrivial AQH phase. When $|M| > |2(t_2 - t_2')|$, m_+ and m_- take the same sign, so the Chern number vanishes and the system lies in the normal band insulator (BI) phase. In the following, we assume $t_2' = -t_2$. In addition, we take t_1 and $\frac{\hbar}{t_1}$ as the unit of energy and time, respectively.

In Eqs. (2) and (3), the low-energy bands around the Dirac points can be obtained directly as:

$$E^{\alpha s}(\mathbf{k}) = s\sqrt{m_\alpha^2 + \frac{1}{2}\hbar^2 v_F^2 k^2}, \tag{4}$$

where $s = +$ $(-)$ means the hole (electron) component. At the Dirac points, the coupling between two sublattices vanishes so that the wavefunctions are also the eigenstates of σ_z and will be localized at sublattice A or B, with the corresponding eigenenergy E_A or E_B. For a given valley, the gap at the Dirac point is:

$$\Delta_\alpha = E_A - E_B = 2m_\alpha. \tag{5}$$

From Eq. (5), we can see that the competition between the staggered onsite energy and anisotropy NNN hopping integrals determines the properties of the wavefunctions at the Dirac points.

In Fig. 2 with the parameters chosen corresponding to the points I and II in Fig. 1(b), the parabolic band structures of the system in both valleys are plot. We can see that in the BI phase,